LIMNOLOGY
and
OCEANOGRAPHY

ASLO

Limnol. Oceanogr. 62, 2017, 1066–1079

doi: 10.1002/lno.10486

Direct measurements of the light dependence of gross photosynthesis and oxygen consumption in the ocean

Benjamin Bailleul,[1,2a] Jisoo Park,[3] Christopher M. Brown,[1] Kay D. Bidle,[1] Sang Hoon Lee,[3] Paul G. Falkowski[1]*

[1]Environmental Biophysics and Molecular Ecology Program, Department of Marine and Coastal Sciences, Rutgers University, New Brunswick, New Jersey
[2]Laboratoire de Génétique des Micro-organismes, Université de Liège, Liège, Belgium
[3]Korea Polar Research Institute, Yeonsu-gu, Incheon, Korea

Abstract

We measured the light dependence of gross photosynthesis and oxygen uptake rates by membrane inlet mass spectrometry in two open ocean regions: the Amundsen Sea (Antarctica), dominated by *Phaeocystis antarctica*, and the North Atlantic, dominated by *Emiliania huxleyi*. In the North Atlantic, respiration was independent of irradiance and was higher than the gross photosynthetic rate at all irradiances. In contrast, in the Amundsen Sea, oxygen uptake processes were light dependent; dark respiration was one order of magnitude lower than the maximal gross photosynthetic rate, but the oxygen uptake rate increased by 10 fold at surface irradiances. Our results suggest the light dependence of oxygen uptake in Amundsen Sea has two sources: one is independent of photosynthesis, and is possibly associated with the photo-reduction of O_2 mediated by dissolved organic matter; the second reflects the activity of an oxidase fueled in the light with photosynthetic electron flow. Our results highlight the importance of improving our understanding of oxygen consuming reactions in the euphotic zone.

Phytoplankton blooms are rare events that play important roles in Earth's natural oceanographic carbon cycle through their contributions to net and export production (Falkowski et al. 2003). By definition, a bloom occurs when net primary production exceeds all loss processes. The vast majority of measurements of oceanic primary production are based on the light dependent incorporation of inorganic radiocarbon into organic matter. It is generally assumed that when integrated over a day or some other convenient time, the results closely reflect net primary production. Although exceedingly sensitive, radiocarbon measurements are inevitably positive and do not reveal any loss processes directly, even during bloom demise.

A clearer measure of net primary production is based on how oxygen is produced and consumed (e.g., Williams et al. 2013). This issue resolves around two processes. On an ecological level, it considers all phytoplanktonic production of oxygen and all loss processes of the gas. On a physiological level it takes into account dark respiration. But a fundamental problem remains; how light-dependent is mitochondrial respiration (and oxygen uptake processes in general) in the real world ocean? A lack of understanding of how oxygen uptake is influenced by light stymies our ability to quantitatively analyze and integrate the in situ allocation of carbon by phytoplankton with the bio-physical mechanisms that allow these organisms to bloom.

Although it has been known for decades that the ratio of photosynthesis to dark respiration varies significantly with growth rate (e.g., Ryther 1954, 1956), respiration is generally assumed to be 10% of maximal gross photosynthesis (Burris 1980) and independent of light (e.g., Falkowski and Owens 1978). However, it has been shown that community respiration increases in response to the "new" carbon produced in the light (Kiddon et al. 1995). Moreover, in photoautotrophs, it is well known that photosynthesis and respiration are coupled on short (millisecond) timescales, with the mode and degree of their interaction varying with the organism and environmental conditions (Healey and Myers 1971). In the light, oxygen consuming processes in the mitochondria (i.e., "dark" respiration) can be enhanced due to the

*Correspondence: falko@marine.rutgers.edu

[a]Present address: Institut de Biologie Physico-Chimique (IBPC), UMR 7141, Centre National de la Recherche Scientifique (CNRS), Université Pierre et Marie Curie, Paris, France

Additional Supporting Information may be found in the online version of this article.

increased availability of photosynthetic products (Falkowski et al. 1985). Other light induced oxygen uptake activities can take place in the plastid, including: (1) the Mehler reaction, which consists of the reduction of O_2 into superoxides on the donor side of photosystem I (Mehler 1957), (2) the oxygenase activity of RuBisCO (ribulose 1,5-bisphosphate carboxylase/oxygenase; Ogren and Bowes 1971), (3) the activity of flavo-di-iron proteins (Allahverdiyeva et al. 2013), and (4) the activity of the plastid terminal oxidase (Bennoun 1982). Those short-term processes result in the biochemical reduction of molecular oxygen by electrons originating from the oxidation of water at the photosystem II (PSII) level, and are therefore known as water-to-water cycles (WWC; Eberhard et al. 2008). As a result of those light-induced oxygen consumption processes, the production of adenosine triphosphate (ATP) relative to Nicotinamide adenine dinucleotide phosphate (NADPH) can be modified (eberhard et al, 2008). On a macroscopic scale, it influences the fate of the bloom by decreasing the net-to-gross (N/G) O_2 production ratio.

Bottle incubations with added isotopic tracers of oxygen (e.g., Bender and Grande 1987), or the use in parallel of O_2-to-Ar ratio measurements and the triple isotope method (e.g., Reuer et al. 2007) improved our estimations of N/G O_2 production ratio in situ. However, because those techniques integrate the gas exchange in the whole community on long timescales (hours or days), it is difficult to distinguish between the WWC and respiration of the community-produced "new" carbon. Moreover, those techniques can be potentially compromised by the photo-reduction of O_2 mediated by organic matter (Amon and Benner 1996).

Efforts to better understand the metabolic coupling between photosynthesis and oxygen uptake in laboratory conditions have relied mostly on membrane inlet mass spectrometry (MIMS, see Beckmann et al. 2009, for a review) and the associated use of oxygen isotopes ($^{18}O_2$). To our knowledge, the only time MIMS has been used in situ is when Kana et al. (1994) investigated the photosynthesis, dark respiration, and light-dependent O_2 uptake in a *Trichodesmium* bloom. Here, we use this methodology to investigate the phytoplankton energetics in situ, and to quantify the importance of light dependent oxygen consumption in two contrasting oceanic regions. We compared the light-dependencies of oxygen gross production and uptake rates over the course of two extensive oceanographic cruises, in two distinct haptophyte blooms during the declining stage: *Emiliania huxleyi* in the North Atlantic and *Phaeocystis antarctica* in the Amundsen Sea, Antarctica.

Study sites and methods

Sampling sites

The *E. huxleyi* samples were harvested toward the end of an extensive bloom (cell concentration reached 4.5×10^3 mL^{-1}) encountered in an anticyclonic eddy during the North Atlantic Virus of Coccolithophore Expedition (NA VICE; KN207-03; http://osprey.bco-dmo.org/project.cfm?flag = view&id = 150) aboard the R/V *Knorr* (*see* Fig. 1A,B; Table 1). The cruise consisted of one transect from Ponta Delgada, Azores to Reykjavik, Iceland from 15 June to 14 July 2012. Given the samples harvested for chlorophyll *a* were lost in Reykjavik, the MIMS data from this cruise were normalized to the maximal rate of gross photosynthesis instead of to chlorophyll.

P. antarctica samples were harvested during a survey in the Amundsen Sea (Amundsen project), conducted between 10 February to 09 March 2012 on the Korean ice-breaker R/V *Araon* (*see* Fig. 1C,D; Table 1). Only stations where we could measure at least two water samples from two different depths within the upper mixed layer are considered in this work.

Mixed layer depths (MLD) were calculated from density profiles based on Conductivity, Temperature, and Depth (CTD) measurements (criterion: 0.05 kg m^{-3} potential density difference to 10 m depth).

Phytoplankton sampling

Water samples were collected using a CTD-Rosette equipped with 10 L Niskin bottles. Water was transferred from the Niskin bottles to 10 L polypropylene carboys, immediately placed in a seawater bath (sea-ice was added in Antarctica). For sea-ice algae, the ice was allowed to thaw in the bath, at 5 ± 2 μmol photons m^{-2} s^{-1}.

Enrichment of phytoplankton cells

Water samples (300 mL) were filtered through Nucleopore 3 μm pore-size membrane filters by gravity or under very low vacuum (< 3 mbar). Cells were resuspended in 3 mL of the original water sample by soaking and gentle shaking in a 50 mL polypropylene centrifuge tube, which was also kept in the seawater bath. The process was repeated 5 to 15 times (for a total duration of no more than 1.5 h) until the sample reached a chlorophyll concentration in the μg/mL range. During the concentration process, light intensity (5 ± 2 μmol photons m^{-2} s^{-1}) and temperature were kept constant (0–0.5°C during R/V *Araon*, or with the R/V *Knorr's* seawater circulation). After the phytoplankton were concentrated, the samples were examined by microscopy (R/V *Araon*) or by flow cytometry (R/V *Knorr*, *see* Supporting Information Fig. 2) to confirm that they were dominated by *P. antarctica* and *E. huxleyi*, respectively. The photo-physiological status was checked by variable chlorophyll fluorescence; in all the samples used for MIMS measurement, the PSII parameters (F_v/F_m, σ_{PSII}, see below) were not affected by the concentration process (Table 1).

Flow cytometry

Cell counts were made with a Millipore Guava easyCyte flow cytometer equipped with a 488 nm laser. The flow

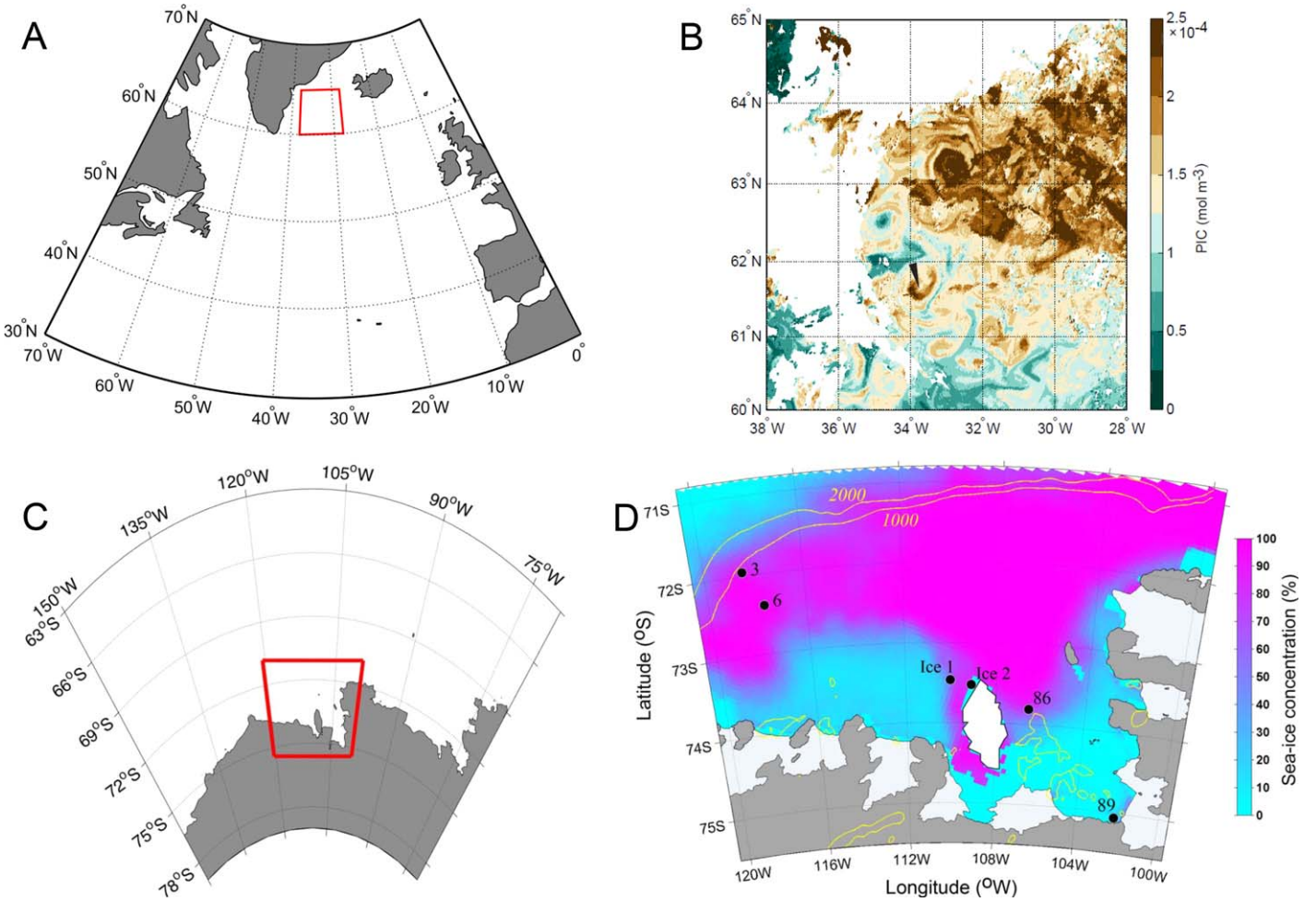

Fig. 1. Locations of the sampling stations in *Emiliania huxleyi* (North Atlantic) and *Phaeocystis antarctica* (Amundsen Sea) blooms. (**A**) Map of sampling area in the North Atlantic cruise. (**B**) MODIS-Aqua satellite data showing PIC (Particulate Inorganic Carbon) signatures (three day averages, spanning 2–4 July 2012) corresponding to the North Atlantic station (Cocco1, designated by black arrow). Sampling stations were inside an anticyclonic eddy feature that contained an *E. huxleyi* bloom undergoing Coccolithovirus infection. Three samplings were done on 2nd July, 7th July, and 9th July (for the exact location of the sampling, *see* Table 1). (**C**) Map of sampling area in the Amundsen Sea. (**D**) Map of the Amundsen Sea with the sea-ice signature (mean sea-ice concentration between 10th February and 9th March 2012) and the locations of the stations (3, 6, 86, 89 and Ice 1 and 2) where *P. antarctica* bloom was harvested. See Table 1 for more information about the sampling locations.

cytometer was bead-calibrated at the start of each experiment for flow rate and concentration. InCyte 2.2.2 software was used to gate and quantify populations. Phytoplankton populations were gated using side scatter and red fluorescence. *E. huxleyi* was gated as a distinct population using forward scatter and side scatter.

Fluorescence parameters

PSII parameters were assessed using a custom-built Fluorescence Induction and Relaxation System (FIRe, Gorbunov and Falkowski 2005). The maximal quantum efficiency of PSII ($F_v/F_m = [F_m - F_o]/F_m$) and the functional absorption cross-section of PSII (σ_{PSII}) were calculated from the analysis of fluorescence induction kinetic profiles on the microsecond time scale on both the concentrated and nonconcentrated samples (Kolber et al. 1998). The concentration process under very low light allows for the complete recovery from potential non photochemical quenching processes. Samples were further acclimated to darkness for 5 min before the FIRe measurements. For the depth-dependencies of PSII parameters (Fig. 3), samples were transferred from Niskin bottles and dark adapted for 30 min in amber bottles.

Membrane inlet mass spectrometer measurements

Rates of O_2 production and uptake were measured using MIMS. The sample was introduced into a 3 mL thermostat-cuvette, which was connected to a Quadrupole Mass Spectrometer (QMS 200, Pfeiffer Vacuum Prisma, Asslar, Germany) by a stainless steel vacuum tube (1/8 inch) passing through a water trap filled with ethanol and dry ice. The concentrated phytoplankton samples were separated from the tube *via* a gas permeable inlet system (PTFE membrane, 0.01 mm). A

Table 1. Sampling locations, nutrients and PSII parameters. The water samples used for nutrient quantification correspond to the water used for the MIMS measurements (see Methods), or to the closest location where it was available (station A and C from North Atlantic, in that case the location of the nutrient measurements is displayed in the orthophosphate column). The PSII parameters were measured before and after the concentration process (see Methods) to demonstrate that the process did not affect the photosynthetic physiology (only the F_v/F_m at Sta. 89 and the cross-section at Sta. 3, 10 m depth, changed by more than 10%).

Station	Latitude; longitude	MLD (m)	Ammonia (μM)	Nitrate/ Nitrite (μM)	Silicate (μM)	Orthophosphate (μM)	Sampling depth (m)	$F_v/F_m/\sigma_{PSII}$ (nm^2) before	$F_v/F_m/\sigma_{PSII}$ (nm^2) after
3 (Fig. 4)	71.95°S;	29	0.50	1.71	68.2	22.14	10	0.39/2.15	0.37/2.97
	118.45°W						20	0.36/2.55	0.33/2.44
6 (Figs. 3, 4)	72.39°S;	28	0.42	1.72	76.8	23.50	5	0.44/2.57	0.41/2.41
	117.72°W						20	0.45/2.83	0.42/2.54
86 (Figs. 2, 3)	73.81°S;	27	1.64	1.43	66.9	15.31	5	0.50/3.03	0.51/2.97
	106.54°W						20	0.49/2.95	0.49/3.09
89 (Fig. 4)	75.06°S;	42	1.60	1.52	59.8	18.24	20	0.48/2.95	0.42/3.11
	102.15°W						40	0.51/2.91	0.43/2.70
3 (Supporting Information Fig. 1)	71.95°S; 118.45°W						20	0.39/2.95	0.44/2.96
63 (Supporting Information Fig. 1)	72.93°S; 117.58°W						20	0.45/2.85	0.45/2.82
Ice 1 (Fig. 4)	73.47°S; 110.037°W							0.11/2.71	0.10/2.93
Ice 2 (Fig. 4)	73.53°S; 109.13°W							0.31/2.40	0.31/2.30
Ice 2 (Supporting Information Fig. 1)	73.53°S; 109.13°W							0.37/2.94	0.35/2.99
A	61.86°N; 33.60°W		0.87	6.75	1.09	0.023 (61.80°N; 33.31°W)	11		
B	61.69°N; 33.78°W		6.88	5.59	0.14	0.013	5		
C	61.86°N; 33.97°W		2.84	4.42	0.555	0.030 (61.80°N; 33.90°W)	9		

mixed $^{18}O_2$-enriched solution was added to obtain a final concentration of $^{18}O_2$ equivalent to 4% to 8% of total O_2, at the beginning of the experiment. The cuvette was sealed and the partial pressures of $^{16}O_2$ ($p(^{16}O_2)$, m/z = 32), $^{18}O_2$ ($p(^{18}O_2)$, m/z = 36) and Ar (p(Ar), m/z = 40) were measured. The concentrations of $^{16}O^{18}O$ and $^{16}O^{17}O$ isotopologues were not taken into account because of their low abundance (only peaks at m/z = 32 and 36 were detected in our experiments).

The MIMS analyses at different irradiances were only performed 1.5 h later, in order to avoid artifacts due to initial gas disequilibration.

A blue LED source, spectrally equivalent to the one used in the FIRe system, and chosen for its resemblance to the natural spectrum at depth in the ocean, was connected to the cuvette. The light intensity was manually adjustable in the 0 to 800 μmol photons m^{-2} s^{-1} range. The light intervals lasted approximately 20 min to allow the cells to photo-acclimate and to ensure a sufficient signal-to-noise ratio. The internal cuvette temperature was kept at 0.3 ± 0.1°C during the Amundsen Sea cruise using a thermostated pump with ethylene glycol added to prevent freezing. During the North Atlantic cruise, the ship's sea water circulation was used to keep the cuvette at ambient surface water temperature.

To calculate gross O_2 production (O_P) and uptake (O_U), the production and consumption by the cells, we adapted the equations from (Peltier and Thibault 1985),

$$O_U = -\left(\Delta[^{18}O_2]/\Delta t + k_{18o}[^{18}O_2]\right) * \left([^{18}O_2]+[^{16}O_2]\right)/[^{18}O_2]$$

$$O_P = \left(\Delta[^{16}O_2]/\Delta t + k_{16o}[^{16}O_2]\right) + O_U * [^{16}O_2]/\left([^{18}O_2]+[^{16}O_2]\right)$$

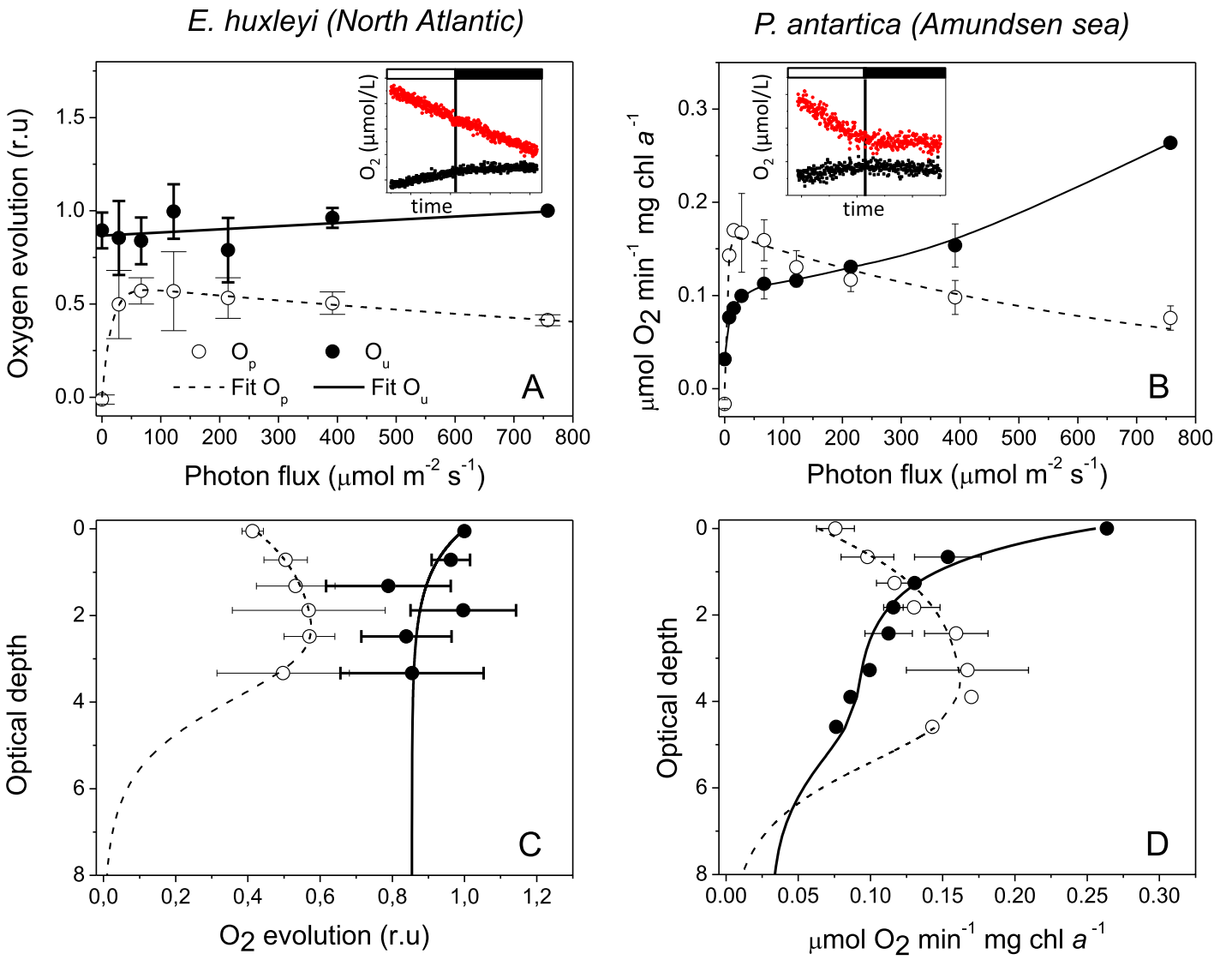

Fig. 2. Light (panel A, B) and depth (panel C, D) dependencies of gross oxygen production and oxygen uptake in *E. huxleyi* and *P. antarctica* blooms. Open circles: O_P, gross oxygen production; closed circles: O_U, oxygen uptake. (**A,C**) Average of three *E. huxleyi* enriched samples (± S.D.) from the sampling station in North Atlantic (Fig. 1 and Table 1). (**B,D**) Average of two *P. antarctica* enriched samples (± S.E.) from Pine Island polynya (Sta. 86, two different depths, see Fig. 1, Supporting Information Fig. 3 and Table 1). Data from Amundsen Sea are normalized per Chl *a*. Data from North Atlantic are normalized to the maximal oxygen uptake rate (see Methods). Dash and continuous lines are the fits for the gross oxygen and oxygen uptake rates data, respectively (see Methods). For the conversion from light to OD dependencies, see Methods. Inserts in **A**–**C** correspond to the evolution of the total O_2 consumed (calculated as the integral of O_U, red) or produced (calculated as the integral of O_P, black) at the transition from the highest light (white bar) to darkness (dark bar).

where k_{18o} and k_{16o} are the rate constants of $^{18}O_2$ and $^{16}O_2$ decrease, respectively, due to MIMS consumption and leaks. The determination of k_{18o} and k_{16o} was done empirically by following the decrease of the $[^{18}O_2]$ and $[^{16}O_2]$ in an isotope enriched media blank. O_P and O_U were used instead of E_0 and U_0, to avoid confusion, E being usually used in oceanography to denote light irradiance. We normalized O_2 to Ar, a biologically inert gas with very similar solubility properties (Craig and Hayward 1987); this decreases the sensitivity of O_2 measurements to fluctuations by approximately 80% (Kana et al. 1994). The gas concentrations were calibrated by measuring air-equilibrated O_2 concentration (stirring deionized water in the open cuvette for at least 5 h) and background O_2 (bubbling with N_2 or adding glucose and glucose oxidase).

When needed, the PSII inhibitor 3-(3,4-dichlorophenyl)−1,1-dimethylurea (DCMU, Sigma-Aldrich), dissolved in ethanol, was added at a final concentration of 20 μM.

In order to assess the overall precision of the MIMS method, we measured four replicates of *P. antarctica* which were acclimated to constant light (5 ± 2 μmol photons m^{-2} s^{-1})

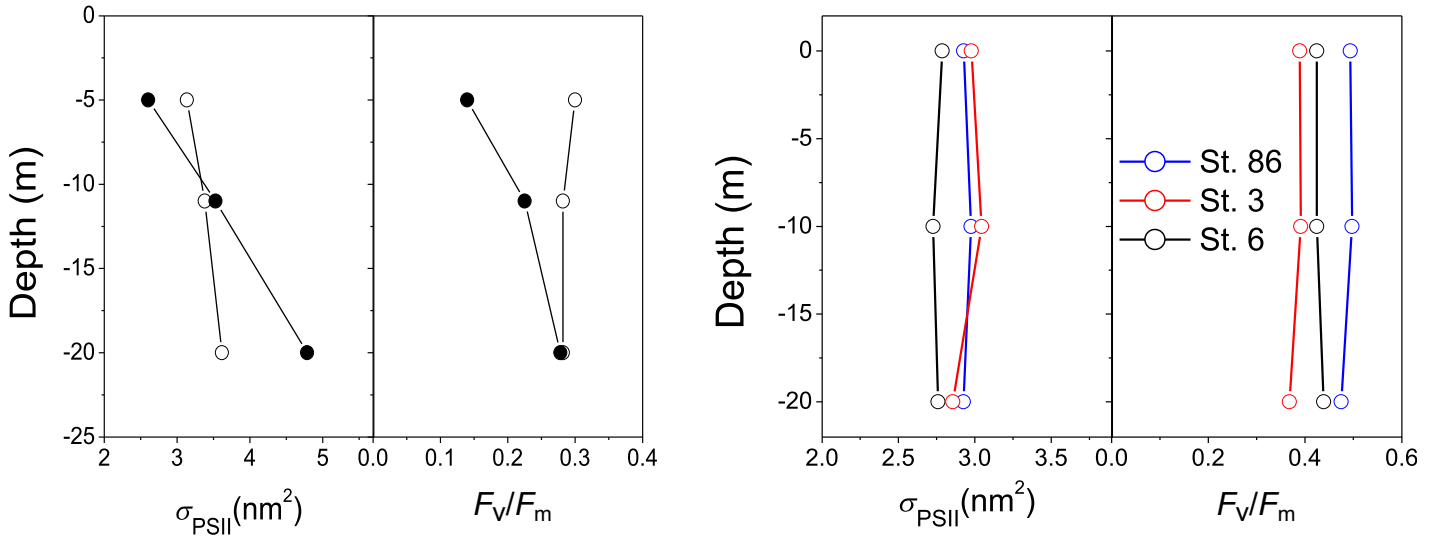

Fig. 3. Depth dependencies of F_v/F_m and σ_{PSII} of *E. huxleyi* and *P. antarctica*. Left panel: depth dependence of F_v/F_m and σ_{PSII} in *E. huxleyi* enriched (retentate, open circles) and non *E. huxleyi* samples (filtrate, closed circles) from North Atlantic. Water samples were first separated on a 3 μm filter (see Methods and Supporting Information Fig. 2) before dark acclimation. Right panel: depth dependence of F_v/F_m and σ_{PSII} from Amundsen Sea (Sta. 3, 6, and 86, note that no significant fluorescence signal could be detected from the filtrate). The PSII parameters were measured on samples from Niskin bottles from the given depth, after dark acclimation over 30 min.

and temperature (0°C, water-ice bath) for 30 h to 42 h to ensure that the physiological state of the cells was the same in successive experiments (Supporting Information Fig. 1A). The water sample (from Sta. 3 and 63) was divided into four volumes of 2 to 3 liters, which were both independently concentrated prior to MIMS measurements. Chlorophyll fluorescence parameters of PSII were checked after concentration (*see* Table 1). The standard deviation of the MIMS experimental data, presented in Supporting Information Fig. 1A, indicate that the precision of the method (0.01 μmol O_2 mg Chl a^{-1} min^{-1}) is sufficient for our purpose.

Extrapolation of the light saturation curves

The oxygen production (O_p) vs. photon flux curves were plotted using the equation from Platt et al. (1980), which takes into account photo-inhibition: $O_P = P_s * (1 - \exp(-\alpha * E/P_s)) * \exp(-\beta * E/P_s)$, where E is the photon flux, P_s is the potential maximal photosynthetic rate, α is the positive slope of curve under light-limited regime, and β is the negative slope of the curve in the high photon flux regime (photo-inhibition parameter). The values given in Table 2 were calculated for each station from the O_P vs. light curve, average of the two samples from two different depths.

The oxygen uptake (O_U) vs. photon flux curves were plotted using the following equation: $O_U = R_d + R_{PSII} * O_P + R_x * E$, where R_d is the dark respiration, R_{PSII} is the ratio of PSII-generated electrons rerouted to O_2, and R_x reflects the quantum yield of O_2 photo-reduction by nonbiological processes. The values given in Table 2 were calculated for each station from the O_U vs. light curve, average of the two samples from two different depths.

Conversion of light dependencies to depth dependencies

The surface photon flux was arbitrarily set to the maximal irradiance in the MIMS cuvette (800 μmol photons m^{-2} s^{-1}, blue light), resembling the maximal sunlight irradiance at the surface of the ocean. Optical depth (OD) was calculated as OD = ln (800/E) with E in μmol photons m^{-2} s^{-1}. At Sta. 86, the attenuation length was 3 m, and the MLD corresponded to 27 m or 9 OD. GPP was calculated by integration of O_P over the mixed layer. NPP was calculated by integrating the difference between O_P and the "biological" oxygen uptake, over the mixed layer.

Phytoplankton growth

For the laboratory measurements, *P. antarctica* was purchased from NCMA (CCMP 1374) and grown in F/2 – Si (Guillard 1975) at 10 μmol photons m^{-2} s^{-1} and 4 ± 1°C. After cells were harvested in exponential phase, the methods were exactly the same as for natural samples, except that the thermostated cuvette of the MIMS was set at 4°C.

Results

Comparative physiologies of *E. huxleyi* and *P. antarctica*

The light dependencies of gross O_2 production (O_P) and uptake (O_U) rates of samples from the North Atlantic dominated by *E. huxleyi* (panel A) and from the Southern Ocean dominated by *P. antarctica* (panel B) are shown in Fig. 2 (*see* also Supporting Information Fig. 3). In *E. huxleyi* samples, O_U was higher than O_P, regardless of light intensity, which led to a negative contribution to net primary productivity. There was no significant light-dependence of O_2 uptake (Fig. 2A), which was highlighted by the unchanged rate of O_2

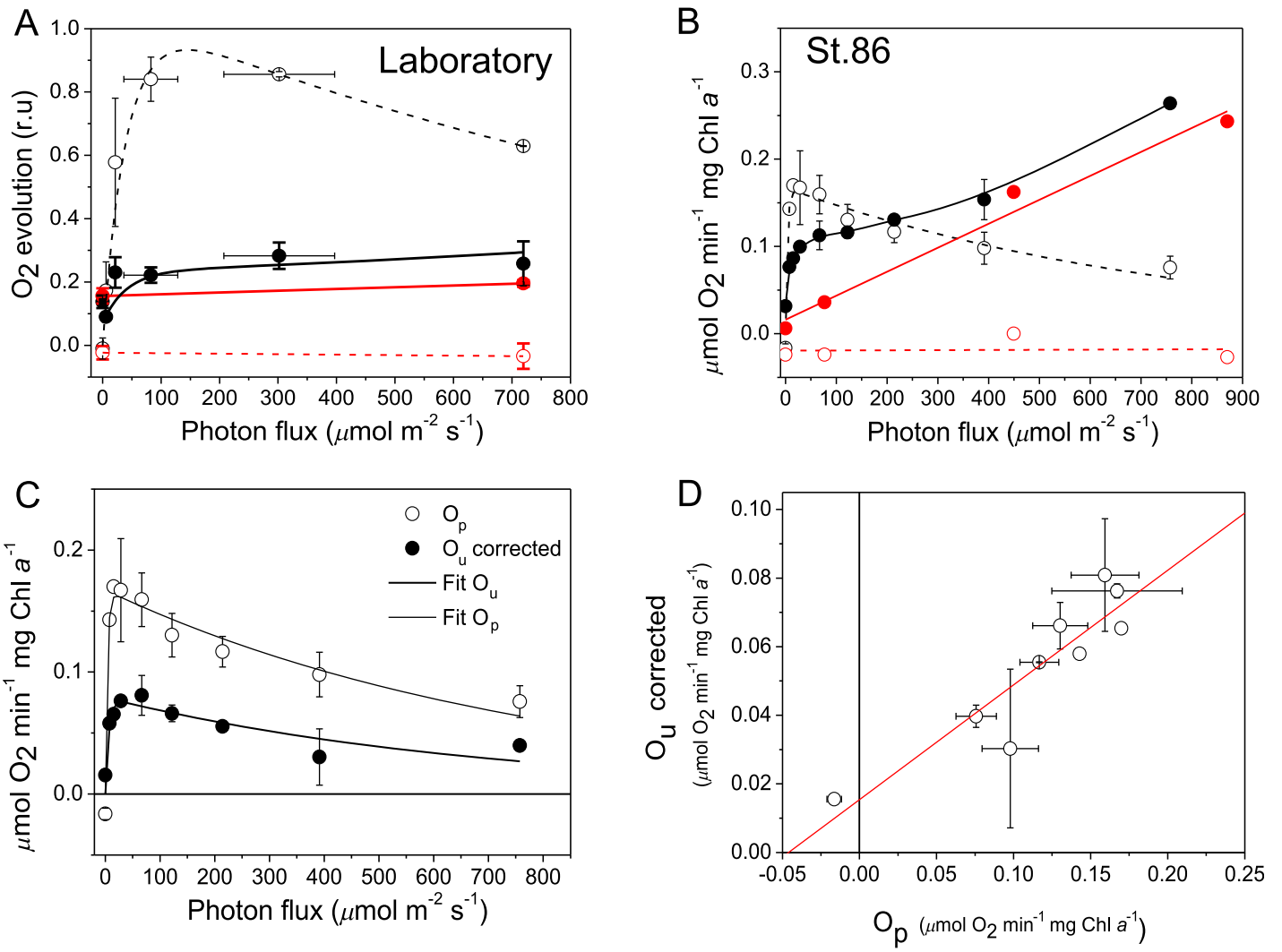

Fig. 4. The three contributions to O_U in *P. antarctica* samples. (**A**) Light dependencies of gross oxygen production (O_P, open symbols) and oxygen uptake (O_U, closed symbols) in *P. antarctica* grown in the laboratory. The data presented correspond to two independent measurements (± S.E.). Black and red symbols correspond to control and DCMU conditions (20 μM), respectively. Black and red lines are fits of the O_P and O_U vs. E data in control and DCMU conditions, respectively (see Methods). Growth conditions are described in Methods. (**B**) Light dependencies of gross oxygen production (O_P, open symbols) and oxygen uptake (O_U, closed symbols) in Sta. 86. (**C**) Light dependencies of gross oxygen production (O_P, open symbols) and corrected oxygen uptake (O_U corrected, closed symbols) in Sta. 86. O_U corrected is obtained by subtracting the non-biological component of O_U (from the linear fit of the DCMU experiment of panel A). (**D**) O_U corrected vs. O_P, using data from panel C (the red line corresponds to a linear fit of the data).

consumption in a light-to-dark transition (*see* insert in Fig. 2A). The situation of *P. antarctica* samples was dramatically different, showing a ~ 10 fold increase in O_U at surface simulated irradiance (760 μmol photons m^{-2} s^{-1}) compared to dark respiration (0.03 ± 0.01 μmol O_2 min^{-1} mg Chl a^{-1}). The transition from highest photon flux to darkness was characterized by the suppression of both the oxygen production and most of its uptake (insert in Fig. 2B). Dark respiration was sixfold lower than maximal photosynthesis. However, the increase of O_U with light, and the concomitant decrease of O_P, reflecting photo-inhibitory processes, led to a situation where the contribution of *P. antarctica* to the O_2 evolution was positive between ~ 5 μmol photons m^{-2} s^{-1} and ~ 200 μmol photons m^{-2} s^{-1}, but negative at the lowest and highest photon fluxes. The light-dependent O_U increase, seemed to be the sum of two contributions: (1) an initial increase from 0 to approximately 25 μmol photons m^{-2} s^{-1}, concomitant with the increase in O_P; and (2) a second increase from 25 μmol photons m^{-2} s^{-1} to 760 μmol photons m^{-2} s^{-1}. The high light-induced O_2 uptake exceeded the maximal O_2 gross production, which ruled out the possibility that the light-dependent consumption of oxygen was entirely driven by photosynthesis. This strikingly contrasted with the observations made on *P.*

Table 2. O_2 gross production and uptake fit parameters. The parameters given in this table originate from the average curve from the two sampling depths at each station, using a fit described by the equations described in Methods: P_s is the potential maximal photosynthetic rate, α is the positive slope of the photosynthesis-irradiance curve under light-limited regime, β is the photo-inhibition parameter. R_d is the dark respiration, R_{PSII} is the rate of PSII-generated electrons rerouted to O_2, and R_x reflects the quantum yield of O_2 photo-reduction by nonbiological processes. Values are given ± standar error.

Station	P_s (μmol O_2 mg Chl a^{-1} min^{-1})	α (μmol O_2 m^2 mg Chl a^{-1})	β (10^{-4} μmol $O_2 m^2$ mg Chl a^{-1})	R_d (μmol O_2 mg Chl a^{-1} min^{-1})	R_{PSII}	R_x (10^{-2} O_2 m^2 mg Chl a^{-1} $quanta^{-1}$)
3 (Fig. 4D)	0.46 ± 0.06	0.018 ± 0.004	3.0 ± 1.7	0.09 ± 0.02	0.50 ± 0.08	3.9 ± 0.2
6 (Fig. 4C)	0.22 ± 0.02	0.013 ± 0.003	2.2 ± 0.9	0.02 ± 0.02	0.76 ± 0.18	2.0 ± 0.2
86 (Figs. 2, 3)	0.17 ± 0.01	0.045 ± 0.014	2.1 ± 0.4	0.03 ± 0.01	0.34 ± 0.07	2.7 ± 1.5
89 (Fig. 4B)	0.09 ± 0.01	0.009 ± 0.002	0	0.04 ± 0.01	0.89 ± 0.16	1.3 ± 0.8
Replicates	0.28 ± 0.01	0.046 ± 0.006	4.2 ± 0.2	0.04 ± 0.01	0.72 ± 0.04	3.5 ± 0.1
Ice (Fig. 4A)	0.50 ± 0.04	0.025 ± 0.005	2.2 ± 1.3	0.54 ± 0.07	0.13 ± 0.20	4.8 ± 0.8
Ice (Supporting Information Fig. 1)	1.13 ± 0.06	0.094 ± 0.013	3.7 ± 1.6	0.65 ± 0.11	0	5.5 ± 1.2

antarctica grown in the laboratory (Fig. 4A), where only a modest (twofold) increase of oxygen uptake was observed in the light, and where the maximal O_2 gross production rate largely exceeded the maximal oxygen uptake rate.

Obviously, results from a sample from a given depth cannot a priori be generalized to the whole population in the water column, unless all the cells have the same physiology at different depths. In both the Amundsen Sea and North Atlantic stations, the euphotic zone was comprised within the upper mixed layer, allowing constant physicochemical properties of water, with the exception of irradiance. Moreover, in this study, the fluorescence parameters of PSII associated with the haptophytes (F_v/F_m, σ_{PSII}) were remarkably constant within the euphotic zone (Fig. 3). This suggested that the photo-physiology of the cells was constant within the mixed layer, aside from fast processes of light acclimation. Therefore, the methodology used in this study, i.e., acclimating the phytoplankton-concentrated sample to several light irradiance steps (see Methods), was also a means to investigate the depth-dependence of the photo-physiology of the cells, within the euphotic zone. The panels C and D present the extrapolated OD-dependencies of O_P and O_U for the two algae, where surface photon flux was arbitrarily set to 800 μmol photons m^{-2} s^{-1}, typical of a sunny day (see Methods). Figure 2C indicates that the contribution of *E. huxleyi* samples to net O_2 productivity was negative in the entire upper mixed layer. *P. antarctica* contributed negatively to the net O_2 production below 2 ODs and above 4 ODs (Fig. 2D), gross O_2 production exceeding the oxygen uptake only between 2 and 4 ODs.

Three components of O_2 consumption in the Amundsen Sea

Whether the light-dependent O_2 uptake in the Amundsen Sea corresponded to O_2 consumption mediated by photosynthesis (i.e., WWC) or to O_2 photo-reduction mediated by organic matter, will have different consequences on the fate of the phytoplankton and the N/G ratio. If all of the light-induced O_U corresponds to "photosynthesis independent" O_2 photo-reduction, it will not affect carbon fixation and the best estimation of net productivity will be obtained by subtracting dark respiration from O_P. Conversely, if all of the light-induced O_2 uptake is fueled by photosynthetic electron flow from PSII and diverts it from carbon fixation, net productivity should be calculated as the difference between O_P and O_U (see Discussion). To further determine the nature of the O_U, and to distinguish between PSII-dependent and PSII-independent oxygen uptakes, we used a PSII inhibitor (DCMU, see Methods). In laboratory grown cells (Fig. 4A), the addition of DCMU resulted in the complete inhibition of both the O_2 gross production, and the light dependence of O_2 uptake. The oxygen uptake rate was equal to the dark respiration regardless of light intensity. A different behavior was observed at sea: O_2 uptake still increased with light, when gross photosynthesis was fully suppressed by DCMU (Fig. 4B). Nevertheless, the addition of DCMU changed the shape of the light saturation of O_U, thereby confirming the composite nature of O_U in the light. The O_2 uptake which remained in the presence of DCMU reflected non-photosynthetic oxygen consumption and was proportional to photon flux (Fig. 4B). We therefore conclude that it reflected photochemical reaction involving oxygen reduction and organic matter (see Discussion). At the contrary, the low light increase of O_U (in the 0 to 25 μmol photons m^{-2} s^{-1} range) disappeared in the presence of DCMU (Fig. 4B). Moreover, once corrected for the non-photosynthetic oxygen uptake, O_U showed a very similar light-dependence as O_P (Fig. 4C), as expected for a photosynthesis-driven oxygen uptake. A plot of one against the other led to a linear relationship (Fig. 4D),

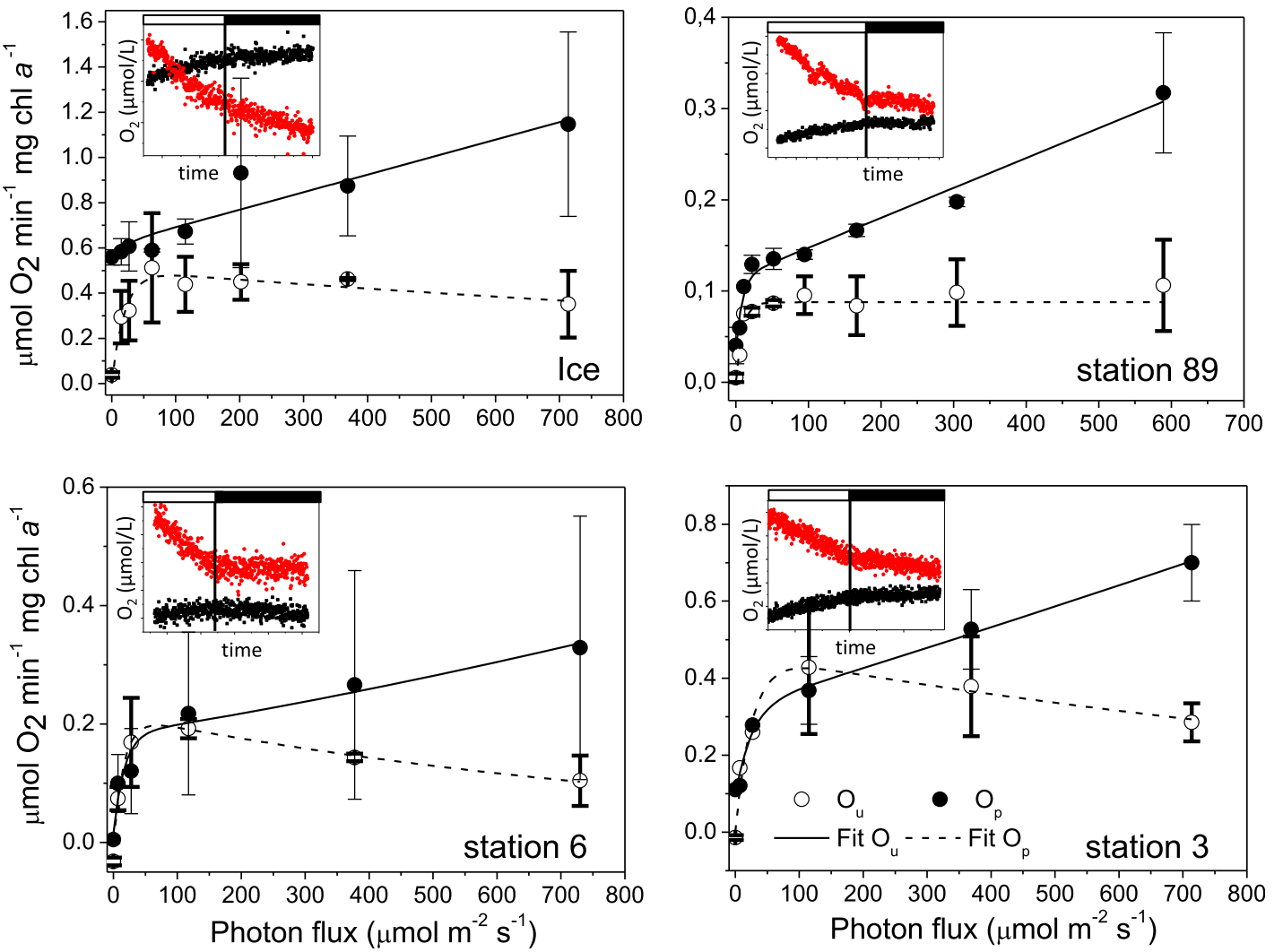

Fig. 5. Light dependencies of gross oxygen production (O_P, open circles) and oxygen uptake (O_U, closed circles) in different regions of Amundsen sea. The four panels correspond to the average of two (± S.E.) *P. antarctica* enriched samples originating from ice (*see* also Supporting Information Fig. 4A) or Sta. 89 (*see* also Supporting Information Fig. 4B), Sta. 6 (*see* also Supporting Information Fig. 4C) and Sta. 3 (*see* also Supporting Information Fig. 4D). Inserts show the kinetics of the total oxygen produced (black) and consumed (red) at the offset of the maximal photon flux. Error bars correspond to standard error. Dash line and bold line are the fit of the gross photosynthesis and oxygen uptake data, respectively (see Methods).

which indicated that the photosynthesis-driven oxygen uptake corresponded to the rerouting of a constant portion of the PSII electron flow to an oxidase. These results indicate that O_U is comprised of three components: (1) a constant dark respiration (R_d), (2) a photosynthesis-independent contribution, which was proportional to photon flux (R_x * E), and (3) a photosynthesis-driven contribution which was proportional to O_P (R_{PSII} * O_P). This interpretation was supported by the strong fit of the O_U vs. E relationship by the sum of those three components at this station (Fig. 4B), as well as in the other stations (Fig. 5 and Supporting Information Fig. 4). This model, when applied to our experimental data from Sta. 86, indicated that a third of the electrons from PSII were rerouted to an oxidase (Fig. 4B; Table 2).

Ice-associated vs. open water *P. antarctica* cells

We also investigated the energetics of *P. antarctica* in four distinct environmental conditions within the Amundsen Sea: a coastal region (Fig. 5B), a sea-ice region (Fig. 5C), an open ocean region (Fig. 5D), as well as cells embedded in the ice (Fig. 5A, see Methods for sampling and thawing). In the open water samples (Fig. 5B–D), maximal oxygen gross production ranged from 0.09 ± 0.01 μmol O_2 mg Chl a^{-1} min^{-1} to 0.46 ± 0.06 μmol O_2 mg Chl a^{-1} min^{-1}. In contrast with the variability in photosynthetic efficiency, the light-

dependence of O_2 uptake showed very similar trends to that observed in the center of the Pine Island polynya. First, high light O_2 uptake was one order of magnitude higher than dark respiration (Fig. 5B–D) and exceeded O_2 gross production, which resulted in net oxygen consumption at surface-simulated irradiances. Moreover, in all open water samples, the strong fit of the experimental data with the model described previously confirmed that (1) the low light increase of O_U corresponded to photosynthesis-driven oxygen uptake, and (2) the further increase was independent of photosynthesis and proportional to irradiance. The contribution of photosynthesis-driven oxygen uptake was higher than for Sta. 86, ranging from 0.50 ± 0.08 (Sta. 3) to 0.89 ± 0.16 (Sta. 89) (*see* Table 2), which indicated that a large proportion of electrons generated in PSII were rerouted to an oxidase rather than carbon fixation. Interestingly, the behavior of ice-originating *P. antarctica* cells was extremely different (Fig. 5A). The dark respiration was one order of magnitude higher than in open water cells (see R_d column in Table 2). Moreover, O_2 uptake increased linearly with photon flux, and there was no concomitant increase of O_U and O_P. This observation, which translated into low values of R_{PSII} in our fitting model, indicated the absence of photosynthesis-driven oxygen uptake in these samples (*see* Table 2 for quantifications of R_{PSII} and other fitting parameters). The maximal photosynthesis was high in those samples (*see* Table 2). Both dark respiration and maximal gross O_2 production further increased with longer incubation, but photosynthesis-driven oxygen uptake was still absent (Supporting Information Fig. 1B).

Discussion

The Amundsen Sea open waters were largely dominated by *P. antarctica* colonies, in agreement with previous reports (Alderkamp et al. 2012). The photosynthesis-irradiance curves of *P. antarctica* samples from Amundsen Sea reveal a low light acclimation, reflected by a light saturation irradiance below 25 μmol photons m^{-2} s^{-1} ($E_k = P_s/\alpha$, from Table 2). The rather constant absorption cross-section of PSII (2.7 nm^2 to 3 nm^2) allows for calculation of the capacity of electron transfer rate from PSII. At light saturation, PSII transfers fewer than 40 electrons per second (σ_{PSII} * E_k). This low value most likely reflects diffusion limitation of the electron transfer reactions in the cold Southern Ocean waters. It was shown recently that the slow rate of carboxylation of RubisCo constrains the carbon fixation in the cold waters of the Western Antarctic Peninsula (Young et al. 2015). However, despite similar temperature conditions in all samples measured, the maximal O_2 gross production can vary by one order of magnitude, from 0.09 ± 0.01 μmol O_2 mg Chl a^{-1} min^{-1} to 1.13 ± 0.06 μmol O_2 mg Chl a^{-1} min^{-1} (Table 2). This indicates that the rate of the limiting step of electron transfer downstream of PSII is limited by other factors. In conditions where the electron transfer rate to carbon fixation is constrained, a common strategy within photosynthetic organisms is to reroute electrons generated by PSII to an oxidase (Eberhard et al. 2008). The PSII-dependent increase of oxygen uptake, concomitant with photosynthesis in the 0-μmol photons m^{-2} s^{-1} to 25-μmol photons m^{-2} s^{-1} range, reveals the existence of such a photosynthesis-driven oxygen uptake in all the open water *P. antarctica* samples. The low resolution of the light-limited regime in our MIMS data and the precision of the method (see Supporting Information Fig. 1 and Methods) may affect the absolute accuracy of the estimation of R_{PSII}. However, the data presented here indicate that a significant portion of PSII electrons ($62 \pm 25\%$, average of Sta. 3, 6, 86, and 89) were rerouted to an oxidase. Regardless of whether the final oxidase is in the mitochondria or plastid, the associated O_2 uptake involves electrons originating from PSII and therefore reflects a WWC. This is in striking contrast with *E. huxleyi* samples where no such WWC was detected. In those samples, respiration is higher than the maximal O_2 gross production, resulting in a negative contribution to net O_2 production in the bloom. This high respiration rate clearly indicates the final phase of the bloom the cells are literally respiring themselves to death. This could be caused by the depletion of nutrients (phosphate concentrations were below 0.03 μM at the surface, and N/P ratios were > 100, *see* Table 1) or by viral infection (Supporting Information Fig. 5). An intermediate observation between the *P. antarctica* and *E. huxleyi* cases investigated here was made by Kana et al. (1994) in a *Trichodesmium thiebautii* bloom. The oxygen uptake in the light increased and this increase, suppressed by DCMU, led to a threefold higher oxygen uptake under high light compared to its dark value.

The WWC was absent from ice-originated *P. antarctica* cells, and the comparison between those cells and their open water counterparts can therefore elucidate the physiology of *P. antarctica*. The O_2-based gross production is higher in ice-originating cells (0.71 ± 0.36 μmol O_2 mg Chl a^{-1} min^{-1}, $n = 3$) compared to open water cells (0.23 ± 0.16 μmol O_2 mg Chl a^{-1} min^{-1}, $n = 8$). Moreover, the absence of WWC indicates that ice-originated cells use all the electrons generated by PSII for carbon fixation and nitrate reduction, whereas only 38% (average on four stations) are used for those purposes in the open ocean. One could expect that the higher carbon assimilation capacity translates into the rise of the substrate availability for Krebs cycle, which is indeed indicated by the 10 fold higher dark respiration compared to open water cells. In the latter, a WWC will generate a proton gradient, which will in turn provide extra ATP without providing NADPH (Eberhard et al. 2008), potentially compensating for the low ATP generated by dark respiration. Another potential advantage of WWC pertains to a role in photoprotection of PSII, by providing a supplementary "well" for the PSII-generated electrons (Eberhard et al. 2008). However, this well represents only a part of a PSII activity, which we

estimated to tens of electrons per second, whereas the absorption of cells at the surface of the Ocean on a sunny day (E = 800 μmol photons m^{-2} s^{-1}) might reach up to approximately 1200 photons per second (σ_{PSII} * E). It is therefore unlikely that the WWC plays any significant role in photo-protection in these cold waters. The occurrence of WWC in open water algae might reflect the rerouting of electrons, upwards CBB cycle, when its capacity constrains the electron flow from PSII, and the generation of extra ATP when mitochondrial respiration is limited by the subsequent low Krebs cycle activity. The different carbon fixation capacities in *P. antarctica*, coming from ice or water, despite similar absorption cross-sections for PSII, suggests that they are prone to a different nutrient availability (Supporting Information Fig. 6; see also Ducklow et al. 2015). The large variability in photosynthetic efficiencies was not reflective of macronutrient limitation (Table 1). In the Southern Ocean, the algal production is clearly prone to iron-limitation (e.g., Martin et al. 1990; Boyd et al. 2000). It was shown that melting sea-ice was a major source of dissolved iron in these waters (Sedwick and DiTullio 1997; Gerringa et al. 2012). We therefore propose that the different productivity of ice-originating and open waters *P. antarctica* may have resulted from a different iron cell status.

In addition to the WWC, a second contribution to the light-induced oxygen uptake was detected for *P. antarctica* in all samples, which did not depend on photosynthesis and increased linearly with light irradiance. We cannot rule out the hypothesis of a direct (photosynthesis independent) light regulation of the mitochondrial respiration. This was proposed earlier (Weger et al. 1989) but, to our knowledge, such a regulation has not been previously documented. It seems more likely that this contribution reflects photochemical reaction involving oxygen reduction and organic matter. The organic matter involved in O_2 photo-reduction is associated with cells, since it was not detected in filtered seawater. The organic matter involved could be external to the cells (e.g., the polysaccharide matrix that aggregates *P. antarctica* into colonies) or internal to the cells (e.g., chlorophyll, especially PSII reaction center in triplet states $^3P^*_{680}$; Asada 1996). Here, the amplitude of the photo-reduction of O_2 mediated by organic matter is equivalent or exceeds maximal gross production. However, this observation suggests the possibility that these processes might potentially compromise the estimation of the O_2-based net and gross productions from bottle incubations with oxygen isotopes. Indeed, oxygen consumption in the surface layer of oceans associated with photochemical processes can be of the same order of magnitude as the oxygen production by photosynthesis (Gieskes et al. 2015).

Critical depth and N/G productivities

The results from this study highlight the importance of obtaining accurate estimations of the light dependence of oxygen consumption not only for understanding the physiology of phytoplankton in situ, but also estimation of the critical depth and of the net-to-gross (N/G) production ratio, both of which play a crucial role in the fate of blooms. The critical depth is at the basis of the standard model of the onset of blooms and is defined as the maximal depth for which the integrated net photosynthesis becomes superior to losses (Sverdrup 1953). *Sensu stricto*, its evaluation requires knowledge of all contributions to losses, including grazing or cell sinking (Smetacek and Passow 1990), but we will assume here that losses are only due to cellular oxygen consumption. The net O_2 production by *P. antarctica* in the water column is the difference between O_2 gross production and O_2 consumption by metabolic processes, which includes dark respiration and light-driven oxygen consumption but not photo-reduction of O_2 mediated by organic matter. Here, we will illustrate the importance of the light dependence of oxygen consumption on the fate of blooms by calculating its influence on the critical depth and N/G production ratio in Sta. 86 in Amundsen Sea (Figs. 1B, 3). Three different situations can be drawn, depending on the nature of the three contributions to O_2 uptake (Fig. 6; see Material and methods). If we consider that only the dark respiration is a biological process, the critical depth and N/G O_2 production should be calculated on the basis of the gross photosynthesis (O_P) and dark respiration (R_d, *see* Fig. 6A,B, green lines), which leads to values of 28 OD and 0.69, respectively (green line and arrow in Fig. 6C, green columns on Fig. 6D; see Methods for calculation). At the other extreme, if all the O_2 uptake corresponds to metabolic processes, the two parameters should be calculated on the basis of O_P and O_U (red line, Fig. 6A,B), which leads to values of 12 OD and 0.11 (red line and arrow in Fig. 6C, red columns in Fig. 6D). An intermediate situation seems more realistic, in which we assess the low light increase of O_U, concomitant to O_P, to WWC, and the high light increase, proportional to photon flux, to photo-reduction of organic matter. Accordingly, only the dark respiration and the WWC (photosynthesis-dependent contribution to light-induced O_2 uptake) correspond to metabolic processes and should be taken into account as losses (blue line, Fig. 6A,B). This leads to a value of 18 OD for the critical depth and 0.35 for N/G O_2 production (blue line and arrow in Fig. 6C, blue columns in Fig. 6D). The wide gap between the values for critical depths and N/G O_2 production based on the three cases described above reflects the importance of a proper assessment of the biological oxygen uptake for a correct estimation of those parameters. The important impact of the photosynthesis-driven oxygen uptake on critical depth is relevant in the context of the recent work of Behrenfeld (2010), discussing Sverdrup's hypothesis. From analyses of satellite data from the subarctic Atlantic, they suggested that the general assumption that blooms are caused by increased photosynthesis in response to increased irradiance is not strictly true. Rather, they

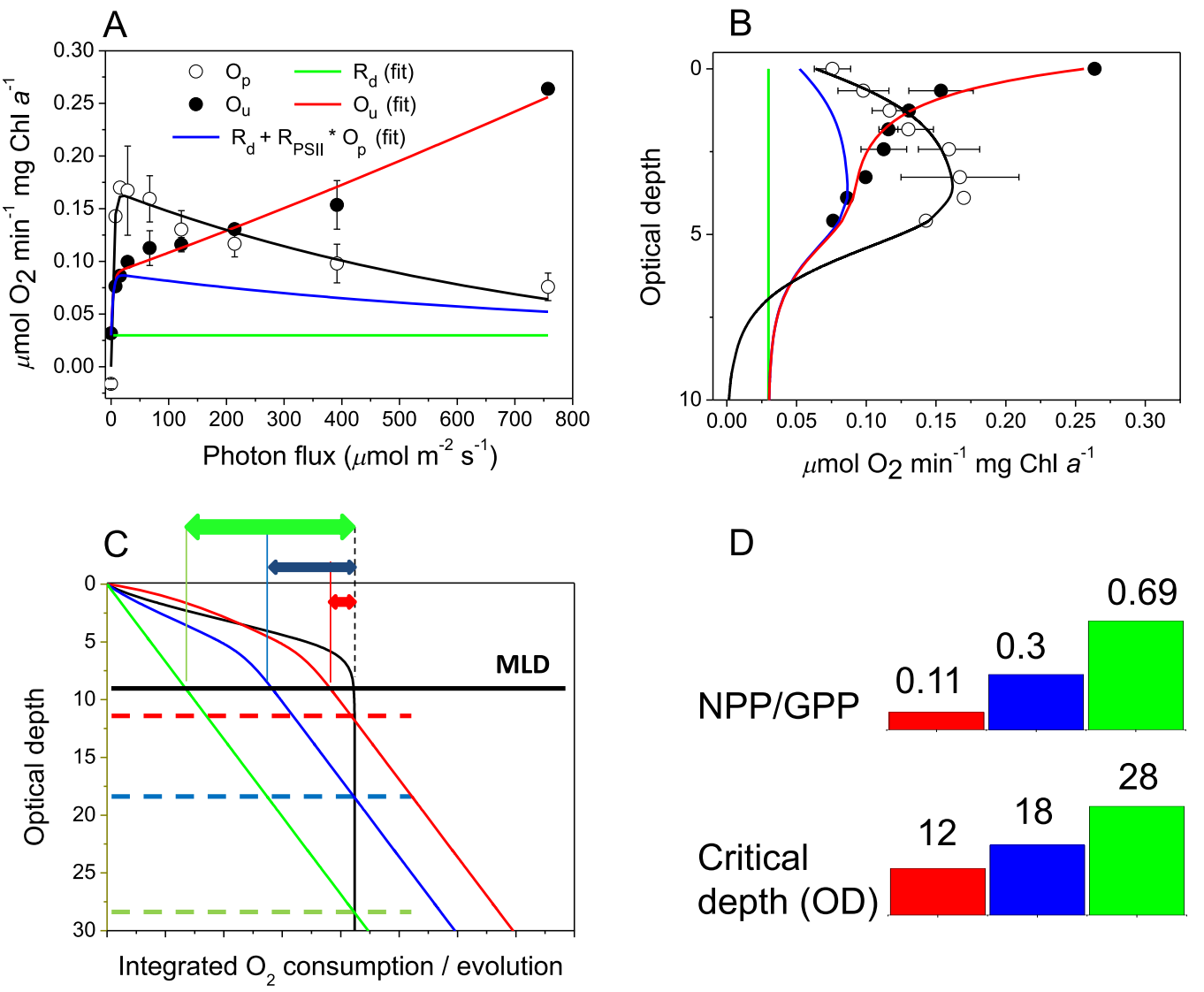

Fig. 6. Calculation of critical depth and N/G production ratio at Sta. 86 (Amundsen Sea). (**A**) Deconvolution of the O_2 uptake into three components. The experimental data for oxygen uptake from Sta. 86 are shown in dark circles and fitted (red line), as the sum of a constant value (dark respiration, green line), a PSII-dependent light-induced oxygen uptake (proportional to O_P, see Methods) and a PSII-independent (DCMU-like) light-induce oxygen uptake (proportional to photon flux, see Material and methods). The blue line corresponds to the sum of dark respiration and the PSII-dependent light oxygen uptake. (**B**) OD profile of gross photosynthesis (open circles) and O_2 uptake (close circles), at Sta. 86. The lines are extrapolated from the sum of the corresponding contributions extrapolated from the model presented in panel A and Material and Methods (*see* also Table 2): only dark respiration (green line), dark respiration + WWC contribution (blue line) or all three components of O_U (red line). (**C**) OD profile of the depth-integrated gross photosynthesis (black line) and oxygen uptake, at Sta. 86. The lines are extrapolated from the sum of the corresponding contributions extrapolated from the model presented in panel A and Material and Methods (*see* also Table 2): only dark respiration (green line), dark respiration + WWC contribution (blue line) or all three components of O_U (red line). Horizontal dashed lines represent the critical depth for each scenario. Vertical lines represent the integrated O_2 metabolic losses (green, blue, red) or production (black) over the MLD for each scenario. Arrows represent the net primary productivity integrated over the MLD for each scenario. (**D**) N/G production ratio and critical depth at Sta. 86 for each scenario.

proposed that blooms might instead be caused by decrease in loss processes, focusing attention on grazing. Obviously, changes in any loss process could explain changes in the critical depth and onset of blooms. The data presented here, gathered during the bloom demise and intense grazing in a complex environment, do not directly resolve this apparent conundrum. However, they indicate that changes in the extent of light dependent oxygen uptake in a water column will clearly modify the critical depth and therefore the calculated net growth of phytoplankton.

References

Alderkamp, A. C., and others. 2012. Iron from melting glaciers fuels phytoplankton blooms in the Amundsen Sea (Southern Ocean): Phytoplankton characteristics and productivity. Deep-Sea Res. Part II Top. Stud. Oceanogr. **71**: 32–48. doi:10.1016/j.dsr2.2012.03.005

Allahverdiyeva, Y., and others. 2013. Flavodiiron proteins Flv1 and Flv3 enable cyanobacterial growth and photosynthesis under fluctuating light. Proc. Natl. Acad. Sci. USA. **110**: 4111–4116. doi:10.1073/pnas.1221194110

Amon, R. M. W., and R. Benner. 1996. Photochemical and microbial consumption of dissolved organic carbon and dissolved oxygen in the Amazon River system. Geochim. Cosmochim. Acta **60**: 1783–1792. doi:10.1016/0016-7037(96)00055-5

Asada, K. 1996. Radical production and scavenging in chloro-plasts, p. 123–150. *In* N. R. Baker [ed.], Photosynthesis and the environment. Kluwer.

Beckmann, K., J. Messinger, M. R. Badger, T. Wydrzynski, and W. Hillier. 2009. On-line mass spectrometry: Membrane inlet sampling. Photosynth. Res. **102**: 511–522. doi:10.1007/s11120-009-9474-7

Behrenfeld, M. J. 2010. Abandoning Sverdrup's critical depth hypothesis on phytoplankton blooms. Ecology **91**: 977–989. doi:10.1890/09-1207.1

Bender, M. L., and K. D. Grande. 1987. Production, respiration, and the isotope geochemistry of O_2 in the upper water column. Glob. Biogeochem. Cycles **1**: 49–59. doi:10.1029/GB001i001p00049

Bennoun, P. 1982. Evidence for a respiratory chain in the chloroplast. Proc. Natl. Acad. Sci. USA. **79**: 4352–4356. doi:10.1073/pnas.79.14.4352

Boyd, P. W., A. J. Watson, C. S. Law, E. R. Abraham, and T. Trull. 2000. A mesoscale phytoplankton bloom in the polar Southern Ocean stimulated by iron fertilization. Nature **407**: 695–702. doi:10.1038/35037500

Burris, J. E. 1980. Respiration and photorespiration in marine algae, p. 411–432. *In* P. G. Falkowski [ed.], Primary productivity in the sea. Plenum Press.

Craig, H., and T. Hayward. 1987. Oxygen supersaturation in the ocean: Biological versus physical contributions. Science **235**: 199–202. doi:10.1126/science.235.4785.199

Ducklow, H. W., and others. 2015. Particle flux over the continental shelf in the Amundsen Sea Polynya and Western Antarctic Peninsula. Elem. Sci. Anth. **3**: 000046. doi:10.12952/journal.elementa.000046

Eberhard, S., G. Finazzi, and F. A. Wollman. 2008. The dynamics of photosynthesis. Annu. Rev. Genet. **42**: 463–515. doi:10.1146/annurev.genet.42.110807.091452

Falkowski, P. G., and T. G. Owens. 1978. Effects of light intensity on photosynthesis and dark respiration in six species of marine phytoplankton. Mar. Biol. **45**: 289–295. doi:10.1007/BF00391815

Falkowski, P. G., Z. Dubinsky, and G. Santostefano. 1985. Light-enhanced dark respiration in phytoplankton. Verh. Internat.Verein. Limnol. **22**: 2830–2833.

Falkowski, P. G., E. A. Laws, R. T. Barber, and J. W. Murray. 2003. Phytoplankton and their role in primary, new, and export production, p. 99–121. *In* M. J. R. Fasham [ed.], Ocean biogeochemistry: The role of the ocean carbon cycle in global change. Springer-Verlag, Berlin, Germany.

Gerringa, L. J., and others. 2012. Iron from melting glaciers fuels the phytoplankton blooms in Amundsen Sea (Southern Ocean): Iron biogeochemistry. Deep-Sea Res. Part II Top. Stud. Oceanogr. **71**: 16–31. doi:10.1016/j.dsr2.2012.03.007

Gieskes, W. W. C., R.W.P.M. Laane, and P. Ruardij. 2015. Photo-oxidation: Major sink of oxygen in the ocean surface layer. Mar. Chem. **177**: 472–475. doi:10.1016/j.marchem.2015.06.003

Gorbunov, M. Y., and P.G. Falkowski. 2005. Fluorescence Induction and Relaxation (FIRe) technique and instrumentation for monitoring photosynthetic processes and primary production. Photosynthesis: Fundamental Aspects to Global Perspectives: Proceedings of the 13th International Congress on Photosynthesis, *In* A. Van der Est and D. Bruce [eds.], Allen and Unwin, London, 1029–1031.

Guillard, R. R. L. 1975. Culture of phytoplankton for feeding marine invertebrates, p. 26–60. *In* W. L. Smith and M. H. Chanley [eds.], Culture of marine invertebrate animals. Plenum Press.

Healey, F. P., and J. Myers. 1971. The Kok effect in Chlamydomonas reinhardi. Plant Physiol. **47**: 373–379. doi:10.1104/pp.47.3.373

Kana, T. M., C. Darkangelo, M. D. Hunt, J. B. Oldham, G. E. Bennett, and J. C. Cornwell. 1994. Membrane inlet mass spectrometer for rapid and high-precision determination of N2, O2, and Ar in environmental water samples. Anal. Chem. **66**: 4166–4170. doi:10.1021/ac00095a009

Kiddon, J., M. L. Bender, and J. Marra. 1995. Production and respiration in the 1989 North Atlantic spring bloom: An analysis of irradiance-dependent changes. Deep-Sea Res. **4**: 553–576. doi:10.1016/0967-0637(95)00008-T

Kolber, Z., O. Prasil, and P. Falkowski. 1998. Measurements of variable chlorophyll fluorescence using fast repetition technique I. Defining methodology and experimental protocols. Biochim. Biophys. Acta **1367**: 88–106. doi:10.1016/S0005-2728(98)00135-2

Martin, J. H., R. M. Gordon, and S. E. Fitzwater. 1990. Iron deficiency limits phytoplankton growth in Antarctic waters. Glob. Biogeochem. Cycles **4**: 5–12. doi:10.1029/GB004i001p00005

Mehler, A. H. 1957. Studies on reactions of illuminated chloroplasts. I. Mechanism of the reduction of oxygen and other hill reagents. Arch. Biochem. Biophys. **33**: 65–77. doi:10.1016/0003-9861(51)90082-3

Ogren, W. L., and G. Bowes. 1971. Ribulose diphosphate carboxylase regulates soybean photorespiration. Nature **230**: 159–160. doi:10.1038/newbio230159a0

Peltier, G., and P. Thibault. 1985. O_2 uptake in the light in Chlamydomonas. Plant Physiol. **79**: 225–230. doi:10.1104/pp.79.1.225

Platt, T., C. L. Gallegos, and W. G. Harrison. 1980. Photoinhibition of photosynthesis in natural assemblages of marine phytoplankton. J. Mar. Res. **38**: 687–701.

Reuer, M. K., B. A. Barnett, M. L. Bender, P. G. Falkowski, and M. B. Hendricks. 2007. New estimates of Southern Ocean biological production rates from O_2/Ar ratios and the triple isotope composition of O_2. Deep-Sea Res. I **54**: 951–974. doi:10.1016/j.dsr.2007.02.007

Ryther, J. H. 1954. The ratio of photosynthesis to respiration in marine plankton algae and its effect upon the measurement of productivity. Deep-Sea Res. **2**: 134–139. doi:10.1016/0146-6313(55)90015-0

Ryther, J. H. 1956. The measurement of primary production. Limnol. Oceanogr. **1**: 72–84. doi:10.4319/lo.1956.1.2.0072

Sedwick, P. N., and G. R. DiTullio. 1997. Regulation of algal blooms in Antarctic shelf waters by the release of iron from melting sea ice. Geophys. Res. Lett. **24**: 2515–2518. doi:10.1029/97GL02596

Smetacek, V., and U. Passow. 1990. Spring bloom initiation and Sverdrup's critical-depth model. Limnol. Oceanogr. **35**: 228–234. doi:10.4319/lo.1990.35.1.0228

Sverdrup, H. U. 1953. On conditions for the vernal blooming of phytoplankton. J. Cons. Int. Explor. Mer. **18**: 287–295. doi:10.1093/icesjms/18.3.287

Weger, H. G., R. Herzig, P. G. Falkowski, and D. H. Turpin. 1989. Respiratory losses in the light in a marine diatom: Measurements by short?term mass spectrometry. Limnology and Oceanography **34**: 1153–1161. doi:10.4319/lo.1989.34.7.1153

Williams, P. J., P. D. Quay, T. K. Westberry, and M. J. Behrenfeld. 2013. The oligotrophic ocean is autotrophic. Ann. Rev. Mar. Sci. **5**: 535–549. doi:10.1146/annurev-marine-121211-172335

Young, J. N., J. A. Goldman, S. A. Kranz, P. D. Tortell, and F. M. Morel. 2015. Slow carboxylation of RubisCo constrains the rate of carbon fixation during Antarctic phytoplankton blooms. New Phytol. **205**: 172–181. doi:10.1111/nph.13021

Acknowledgments

We thank the captain and crew of the R/V *Knorr* and the Marine Facilities and Operations at the Woods Hole Oceanographic Institution for their assistance during the NaVICE Cruise, as well as Jack Di Tullio (College of Charleston, USA) for chlorophyll measurements, and Marco Coolen (Woods Hole Oceanographic Institution, USA; now in Curtin University, Australia) for the EhV virions work (Supporting Information Fig. 5). The project was supported by funding from the National Science Foundation (OCE-1061883 to KDB). We thank the captain and crew of the R/V *Araon* for their assistance during the Amundsen Sea cruise, as well as Mi Sa and Eun Jin Yang (Korea Polar Research Institute) for chlorophyll measurements. J. S. Park and S. H. Lee were, in part, supported by the K-Polar Program (PP13020) of KOPRI. B. Bailleul was supported by a post-doctoral research fellowship from the Institute of Marine and Coastal Sciences, Rutgers University and the Belgian F.R.S.-FNRS (Incentive Grant for Scientific Research F.4520). We thank Ana Martins (University of the Azores, Portugal) and Filipa Carvalho (Rutgers University, USA) for the analysis of the satellite images, K. D. Wyman, Pierre Cardol, Sven Kranz and Tae Siek Rhee for discussions, as well as an anonymous reviewer for comments.

Conflict of Interest

None declared.

Submitted 01 March 2016
Revised 22 July 2016; 09 October 2016
Accepted 14 October 2016

Associate editor: Mikhail Zubkov